

Silicon two-dimensional phononic crystal resonators using alternate defects

Nan Wang,¹ Fu-Li Hsiao,^{1,2} Moorthi Palaniapan,¹ and Chengkuo Lee^{1,a)}

¹Department of Electrical and Computer Engineering, National University of Singapore, Singapore

²Graduate Institute of Photonics, National Changhua University of Education, Taiwan

(Received 26 August 2011; accepted 15 November 2011; published online 5 December 2011)

We present the numerical and experimental investigations of micromechanical resonators made by creating alternate defects with different central-hole radii (r') in a two-dimensional (2-D) phononic crystal (PnC) slab. The PnC structures were fabricated by etching a square array of cylindrical air holes in a $10\ \mu\text{m}$ thick free-standing silicon plate using a CMOS-compatible process. Preliminary experimental results show that the performance of the PnC resonators in terms of resonant frequency, Q factor, and insertion loss (IL) is highly dependent on r' . A Q factor of more than 3000 is achieved for the case of $r' = 6\ \mu\text{m}$ while all the designed resonators with alternate defects have higher Q factor and lower IL than the resonators based on the normal Fabry-Perot structure due to the reduction in the mode mismatch. © 2011 American Institute of Physics. [doi:10.1063/1.3665956]

During the past two decades, propagation of acoustic waves in phononic crystals (PnCs) has received a great deal of attention because of the existence of complete phononic band gaps.^{1–8} Recently, the guided waves in 2-D PnC slabs have attracted more attention due to the fact that the 2-D nature of PnC slabs can provide better confinement of elastic energy. Various configurations of PnC slabs, such as cylindrical air holes etched in freestanding membrane,^{7,8} cylindrical rods inserted into the air holes,⁵ cylindrical rods deposited on the top of the membrane,⁹ as well as inverse acoustic band gap (IABG) structure,¹⁰ have been proved to have phononic band gaps for elastic waves travelling in any direction. By adding defects to PnC structure, devices of various functionalities like waveguides and resonators have been reported.^{9,11–13}

There are many analogies between PnCs and the well-known photonic crystals (PhCs). Due to the strong confinement of light, the optimal PhC cavity can form optical resonators with ultra-high Q factor by modifying rather than simply removing the scatters surrounding or within cavity.¹⁴ The light wave penetrates evanescently into the surrounding PhC when it incidents from the cavity to the surrounding PhC. This leads to significant scattering loss¹⁵ due to the mode mismatch between the cavity mode and the evanescent Bloch mode, i.e., the mode existed in PhC. Therefore, the Q factor is decreased. This can be overcome by varying the scatters between the cavity and the surrounding PhC slightly.^{16,17} The gradual transformation from the cavity mode to the evanescent Bloch mode reduces the scattering loss. Analogically, for Fabry-Perot resonators^{18,19} which experimental investigation of PnC resonators is limited to so far, part of elastic energy is scattered to other directions instead of reflected backward to the incident direction due to the mode mismatch, rendering the reduction of the Q factor.

In this letter, instead of a traditional Fabry-Perot resonator whereby all the central rows of air holes are completely removed, we design and experimentally report PnC resona-

tors with alternate defects. The resonators are made by alternately removing the central four rows of air holes while the radii of the remaining central air holes (r') are varied, and its effect on the performance of the resonators is studied. We also show that by creating alternate defects, the mode mismatch could be decreased resulting in both the enhancement in the Q factor and the reduction in IL, as compared to the Fabry-Perot resonator.

Both the calculation of the band structure and the fabrication process were reported in Ref. 19. Fig. 1 shows the SEM image of microfabricated PnC resonator formed by alternately removing four rows of air holes at the center of the PnC. Inter-digit-transducer electrodes are formed by Al on the two sides of the PnC structure. Four types of r' , including 2, 4, 6, and $8\ \mu\text{m}$, are prepared for the PnC resonators in the current study.

The experimental set-up and characterization methods have also been reported in our previous work.¹⁹ The transmission spectra of the designed resonators are shown in Fig. 2. We observed that the performance of the PnC resonators

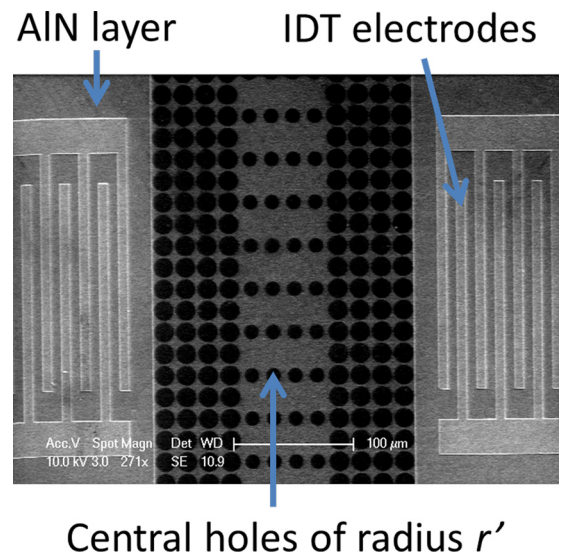


FIG. 1. (Color online) SEM image of microfabricated PnC resonator with alternate defects.

^{a)} Author to whom correspondence should be addressed. Electronic mail: elelc@nus.edu.sg.

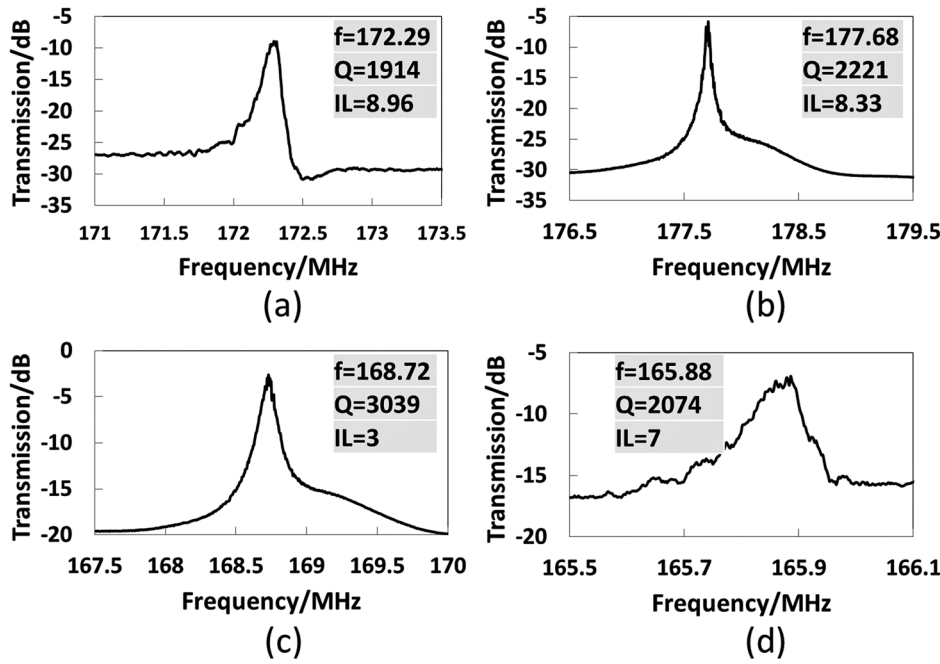


FIG. 2. Measured transmission spectra of PnC resonators with alternate defects and with (a) $r' = 2 \mu\text{m}$ (b) $r' = 4 \mu\text{m}$ (c) $r' = 6 \mu\text{m}$ (d) $r' = 8 \mu\text{m}$. f , Q , IL refer to the resonant frequency, the Q factor, and the insertion loss of the PnC resonator, respectively.

(f , Q , and IL) is highly dependent on r' : f increases from 172.29 to 177.68 MHz as r' increases from 2 to $4 \mu\text{m}$ and drops upon further increment of r' ; Q increases from 1914 to 3039, which is the highest among all the four cases, until r' reaches $6 \mu\text{m}$; IL reduces with the increment in r' until r' reaches $6 \mu\text{m}$ and increases when r' further increases to $8 \mu\text{m}$.

In order to clarify the physical picture of the above four cases, the displacements of steady resonant modes for the four designed resonators are calculated by finite-element-method simulated model and shown in Fig. 3. For the cases whereby the displacement vector components in all three directions are concentrated at the central defect region (e.g., Figs. 3(b) and 3(c)), which means the energy of the structure

is confined and concentrated at the central defect region, a higher Q factor can be obtained. On the other hand, for the cases whereby the displacement vector components are less concentrated at the central cavity region (e.g., Figs. 3(a) and 3(d)), the energy is confined poorly in the central defect region, resulting in a lower Q factor obtained. As the mode of the acoustic phonons are determined by geometric parameters,²⁰ optimization needs to be done in order to get the best slow sound mode, which has the best confinement of acoustic waves. For the four cases with different r' , the case of $r' = 6 \mu\text{m}$ has the best slow sound mode and the mode of acoustic phonons deviates from the optimized resonance condition when r' drifts away from $6 \mu\text{m}$. As such, the quality of confinement of acoustic waves is not in a direct relationship with r' , thus resulting the non-monotonic behavior of the performance parameters as a function of r' .

To further illustrate the difference between the mode shapes of cavity mode and Bloch mode, a Fabry-Perot cavity-mode resonator with four rows of air holes completely removed at the center of the PnC was also analyzed numerically and experimentally. The simulated mode profiles of displacement and the experimentally measured transmission spectrum are shown in Figs. 4(a) and 4(b), respectively. Fig. 4(a) shows the typical Fabry-Perot resonant mode: the elastic energy is uniformly concentrated at the central defect region

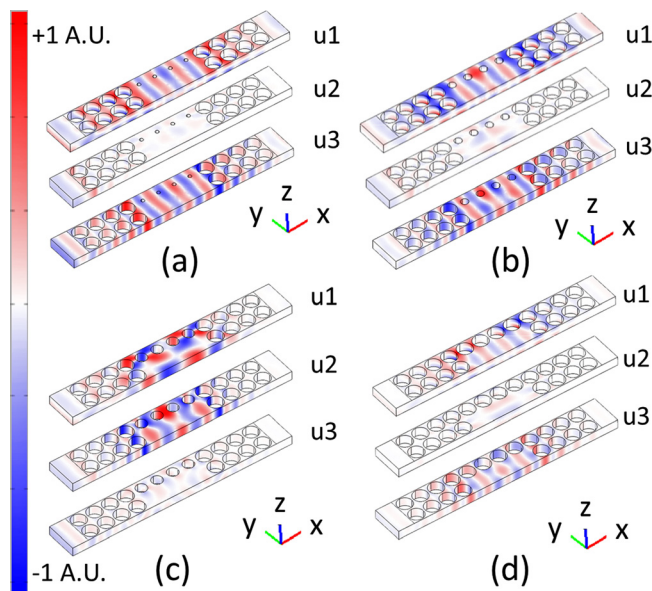


FIG. 3. (Color online) Simulated mode profiles of displacement of PnC resonators with alternate defects and with (a) $r' = 2 \mu\text{m}$ (b) $r' = 4 \mu\text{m}$ (c) $r' = 6 \mu\text{m}$ (d) $r' = 8 \mu\text{m}$. The $u1$, $u2$, and $u3$ represent the displacement vector components in x , y , and z directions, respectively. The color bar indicates the amplitude of displacements in an arbitrary unit.

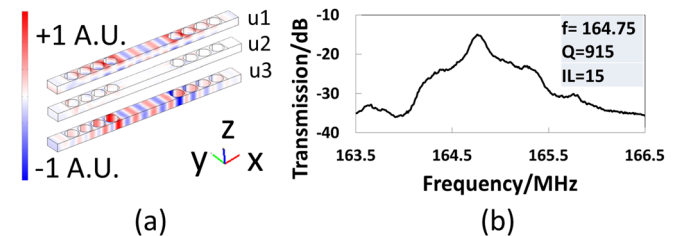


FIG. 4. (Color online) (a) Simulated mode profiles of displacement of the Fabry-Perot resonator. (b) Measured transmission spectrum of the Fabry-Perot resonator.

and the polarization is in x and z directions. The mode is quite similar to the flexural mode of Lamb wave. However, for the proposed resonators with alternate defects, the polarization turns more into y direction as r' increases (Fig. 3) until $6\text{ }\mu\text{m}$, which is the optimized resonance condition with strongest polarization in y direction (Fig. 3(c)). This means that as r' increases, the Lamb-wave mode existed in the case of Fabry-Perot resonator becomes more destroyed by the presence of the alternate defects and eventually becomes a complete non-resonant Bloch mode when $r' = 6\text{ }\mu\text{m}$. In this case, the cavity turns into an oscillator which consists of a mass clamped by the PnC structures on both sides. Hence, part of the incident elastic energy excites the localized mode while another part of the energy excites the propagating mode, which is polarized in y direction and is reflected back and forth within the cavity by the PnC structure surrounding the cavity. This phenomenon is equivalent to the non-resonant propagating mode which exists in the PnC structure surrounding the central cavity and passes through the periodic oscillators array. As such, it is observed that there is a reduction in the mode mismatch existed in the case of traditional Fabry-Perot resonators, which is the mode mismatch between the evanescent propagating mode in the surrounding PnC structure and the resonant cavity mode inside the cavity. Therefore, the gradual transformation from the cavity mode to the evanescent propagating mode reduces the scattering loss, thus enhances Q factor, and reduces IL. From Fig. 4(b), we can see that the Fabry-Perot cavity-mode resonator has a much lower Q factor and a much higher IL as compared to the designed resonators with alternate defects. This agrees with the simulated mode profiles of displacement for both types of resonators. As both types of resonators were fabricated under the same processing conditions, the measured transmission spectra confirm that by having alternate defects at the center of the cavity, the mode mismatch can be reduced thus Q factor and IL can be improved.

In this letter, we experimentally reported the effect of r' on resonant frequency, Q factor, and IL of the PnC resonators with alternate defects in a 2-D PnC slab which is realized from a microfabricated silicon free-standing plate. We found that these parameters are highly dependent on r' , with a Q

factor of more than 3000 achieved for the case of $r' = 6\text{ }\mu\text{m}$. We also show that by creating alternate defects, gradual transformation from the cavity mode to the evanescent propagating mode can be achieved due to the reduction in the mode mismatch between the two modes. As a result, the scattering loss is reduced, leading to the enhancement in both Q factor and IL, as compared to the Fabry-Perot resonator.

This work was supported in research grants of MOE Tier 2 (2009-T2-2011) under WBS: R-263-000-598-112 at the National University of Singapore.

- ¹M. Sigalas, M. S. Kushwaha, E. N. Economou, M. Kafesaki, I. E. Psarobas, and W. Steurer, *Z. Kristallogr.* **220**, 765 (2005).
- ²M. Sigalas and E. N. Economou, *Solid State Commun.* **86**, 141 (1993).
- ³M. S. Kushwaha, P. Halevi, L. Dobrzynski, and B. Djafarirouhani, *Phys. Rev. Lett.* **71**, 2022 (1993).
- ⁴M. S. Kushwaha, P. Halevi, G. Martinez, L. Dobrzynski, and B. Djafarirouhani, *Phys. Rev. B* **49**, 2313 (1994).
- ⁵I. El-Kady, R. H. Olsson, and J. G. Fleming, *Appl. Phys. Lett.* **92**, 233504 (2008).
- ⁶A. Khelif, F. L. Hsiao, A. Choujaa, S. Benchabane, and V. Laude, *IEEE Trans. Ultrason. Ferroelectr. Freq. Control* **57**, 1621 (2010).
- ⁷S. Mohammadi, A. A. Eftekhari, A. Khelif, W. D. Hunt, and A. Adibi, *Appl. Phys. Lett.* **92**, 221905 (2008).
- ⁸T. T. Wu, L. C. Wu, and Z. G. Huang, *J. Appl. Phys.* **97**, 094916 (2005).
- ⁹R. H. Olsson, I. F. El-Kady, M. F. Su, M. R. Tuck, and J. G. Fleming, *Sens. Actuator, A* **145**, 87 (2008).
- ¹⁰N. K. Kuo, C. J. Zuo, and G. Piazza, *Appl. Phys. Lett.* **95**, 093501 (2009).
- ¹¹J. O. Vasseur, A. C. Hladky-Hennion, B. Djafari-Rouhani, F. Duval, B. Dubus, Y. Pennec, and P. A. Deymier, *J. Appl. Phys.* **101**, 114904 (2007).
- ¹²A. Khelif, A. Choujaa, B. Djafari-Rouhani, M. Wilm, S. Ballandras, and V. Laude, *Phys. Rev. B* **68**, 214301 (2003).
- ¹³M. Oudich, M. B. Assouar, and Z. Hou, *Appl. Phys. Lett.* **97**, 193503 (2010).
- ¹⁴T. Tanabe, A. Shinya, E. Kuramochi, S. Kondo, H. Taniyama, and M. Notomi, *Appl. Phys. Lett.* **91**, 021110 (2007).
- ¹⁵P. Lalanne and J. P. Hugonin, *IEEE J. Quantum Electron.* **39**, 1430 (2003).
- ¹⁶P. B. Deotare, M. W. McCutcheon, I. W. Frank, M. Khan, and M. Loncar, *Appl. Phys. Lett.* **94**, 121106 (2009).
- ¹⁷M. W. McCutcheon and M. Loncar, *Opt. Express* **16**, 19136 (2008).
- ¹⁸S. Mohammadi, A. A. Eftekhari, W. D. Hunt, and A. Adibi, *Appl. Phys. Lett.* **94**, 051906 (2009).
- ¹⁹N. Wang, J. M. Tsai, F. L. Hsiao, B. W. Soon, D. L. Kwong, M. Palaniapan, and C. Lee, *IEEE Electron Device Lett.* **32**, 821 (2011).
- ²⁰V. Laude, J. C. Beugnot, S. Benchabane, Y. Pennec, B. Djafari-Rouhani, N. Papanikolaou, J. M. Escalante, and A. Martinez, *Opt. Express* **19**, 9690 (2011).